ELSEVIER

A family of *n*-scroll hyperchaotic attractors and their realization

Simin Yu [a], Jinhu Lü [b,c,e,*], Guanrong Chen [d]

[a] *College of Automation, Guangdong University of Technology, Guangzhou 510090, PR China*
[b] *Key Laboratory of Systems and Control, Institute of Systems Science, Academy of Mathematics and Systems Science, Chinese Academy of Sciences, Beijing 100080, PR China*
[c] *State Key Laboratory of Software Engineering, Wuhan University, Wuhan 430072, PR China*
[d] *Department of Electronic Engineering, City University of Hong Kong, Hong Kong, PR China*
[e] *Department of Ecology and Evolutionary Biology, Princeton University, Princeton, NJ 08544, USA*

Abstract

A systematic circuit design approach is proposed for experimental verification of hyperchaotic 2-, 3-, 4-scroll attractors from a generalized Matsumoto–Chua–Kobayashi (MCK) circuit. Moreover, using appropriate discrete and extended transformations, a novel digital signal processor (DSP) method is also presented for physically realizing the above hyperchaotic 2-, 3-, 4-scroll attractors. This is the first time in the literature to report the experimental verification of hyperchaotic 3- and 4-scroll attractors. Some recursive formulas of system parameters are rigorously derived, useful for improving circuit implementation.
© 2006 Elsevier B.V. All rights reserved.

1. Introduction

Chaos has been intensively investigated over the last four decades [1–23]. Especially, hyperchaos attracted increasing attention in the last few years [4–8,11,21]. Hyperchaos was firstly observed from a real physical system by Matsumoto, Chua and Kobayashi [4,23]. Then, Yalcin and his colleagues introduced some hyperchaotic *n*-double-scroll chaotic attractors by adding breakpoints in the piecewise-linear (PWL) characteristic of the MCK circuit and confirmed the hyperchaotic 4- and 6-scroll attractors by computer simulations [5]. Yu and his colleagues also proposed hyperchaotic *n*-scroll attractors and realized hyperchaotic 3–10-scroll attractors by computer simulations [6]. Itoh and his colleagues investigated the impulsive synchroniza-

tion of a hyperchaotic double-scroll attractor and its application to spread-spectrum communication systems [7].

It has been known that it is much more difficult to realize multi-scroll chaotic and hyperchaotic attractors by electronic circuits [11,12,21]. Yalcin and his colleagues experimentally confirmed 3- and 5-scroll chaotic attractors in a generalized Chua's circuit [8], while Zhong and his colleagues proposed a systematical circuitry design method for physically realizing up to as many as ten scrolls visible on the oscilloscope [12]. Han and his colleagues constructed a double-hysteresis building block to physically realize a 9-scroll chaotic attractor [14]. There are some other approaches reported in the literature for the design and circuit implementation of multi-scroll chaotic attractors [10,11,15–21]. It is generally quite difficult to physically realize a nonlinear resistor having an appropriate characteristic with many segments. The main obstacle is that the device must have a very wide dynamic range [11,12,21], however, physical conditions always limit or even prohibit such circuit realization [12].

---

* Corresponding author.
 E-mail addresses: jhlu@iss.ac.cn (J. Lü), gchen@ee.cityu.edu.hk
(G. Chen).

In this Letter we describe the design of a novel block circuit diagram to experimentally confirm hyperchaotic n-scroll attractors. Furthermore, using appropriate discrete and extended transformations, a novel DSP method is developed to physically realize the above hyperchaotic 2-, 3-, 4-scroll attractors. In particular, this is the first time in the literature to report the experimental verification of hyperchaotic 3- and 4-scroll attractors. Finally, the derived recursive formulas of system parameters provide a theoretical basis for physical circuit realization of hyperchaotic attractors with a large number of scrolls.

2. Theoretical design of n-scroll hyperchaotic attractors

The dimensionless state equation of the hyperchaotic MCK circuit [6,23] is described by

$$
\begin{cases}
\frac{dx}{d\tau} = \alpha[g(y-x) - z], \\
\frac{dy}{d\tau} = \beta[-g(y-x) - w], \\
\frac{dz}{d\tau} = \gamma_0(x+z), \\
\frac{dw}{d\tau} = \gamma y,
\end{cases}
\tag{1}
$$

where $g(y-x) = m_1(y-x) + 0.5(m_0 - m_1)[|y-x+x_1| - |y-x-x_1|]$ is an odd characteristic function. When $\alpha = 2$, $\beta = 20$, $\gamma_0 = 1$, $\gamma = 1.5$, $m_0 = -0.2$, $m_1 = 3$, $x_1 = 1$, system (1) has a hyperchaotic double-scroll attractor [4,6,23].

To generate hyperchaotic n-scroll attractors from (1), one first needs to generalize the characteristic function $g(y-x)$ as follows [6]:

$$
\begin{aligned}
g(y-x) = {}& m_{N-1}(y-x) \\
& + \frac{1}{2} \sum_{i=1}^{N-1} (m_{i-1} - m_i) \\
& \times \left(|y-x+x_i| - |y-x-x_i| \right).
\end{aligned}
\tag{2}
$$

It can be easily verified that the recursive formulas of positive switching points x_i $(i = 2, 3, \ldots, N-1)$ can be deduced as follows:

$$
\begin{cases}
x_2 = \frac{(1+k_1)\sum_{i=1}^{1}(m_i - m_{i-1})x_i}{m_1 - 1} - k_1 x_1, \\
x_3 = \frac{(1+k_2)\sum_{i=1}^{2}(m_i - m_{i-1})x_i}{m_2 - 1} - k_2 x_2, \\
\vdots \\
x_{N-1} = \frac{(1+k_{N-2})\sum_{i=1}^{N-2}(m_i - m_{i-1})x_i}{m_{N-2} - 1} - k_{N-2} x_{N-2},
\end{cases}
\tag{3}
$$

where m_i $(0 \leqslant i \leqslant N-1)$ are the slopes of the segments and radials in various PWL regions, and $k_i = \frac{x_{i+1} - x_i^E}{x_i^E - x_i}$ $(1 \leqslant i \leqslant N-2)$, in which x_i^E $(1 \leqslant i \leqslant N-2)$ are the positive equilibrium points of $g(x)$.

To limit the hyperchaotic signal into the region of the operational amplifier, one may assume that $x_1 < 1$. Here, suppose that $x_1 = 0.5$. From (3), one determines the system parameters as follows: (i) when $N = 2$, $m_0 = -0.2$, $m_1 = 3$, system (1) with (2) has a hyperchaotic double-scroll attractor with Lyapunov exponent spectrum: $LE_1 = 0.240$, $LE_2 = 0.060$, $LE_3 = 0$, $LE_4 = -53.800$, as shown in Fig. 1(a); (ii) when $N = 3$,

$m_0 = 3$, $m_1 = -0.8$, $m_2 = 3$, $k_1 = 1.4$, $x_2 = 1.8333$, system (1) with (2) has a hyperchaotic 3-scroll attractor with Lyapunov exponent spectrum: $LE_1 = 0.247$, $LE_2 = 0.066$, $LE_3 = 0$, $LE_4 = -54.000$, as shown in Fig. 1(b); (iii) when $N = 4$, $m_0 = m_2 = -0.7$, $m_1 = m_3 = 2.9$, $k_1 = 1.3$, $k_2 = 1.3$, $x_2 = 1.5289$, $x_3 = 3.0239$, system (1) with (2) has a hyperchaotic 4-scroll attractor with Lyapunov exponent spectrum: $LE_1 = 0.253$, $LE_2 = 0.070$, $LE_3 = 0$, $LE_4 = -53.600$, as shown in Fig. 1(c).

According to (3), one can easily get the recursive formulas of positive equilibrium points x_i^E $(i = 1, 2, \ldots, N-1)$ as follows:

$$
\begin{cases}
x_1^E = \frac{\sum_{i=1}^{1}(m_i - m_{i-1})x_i}{m_1 - 1}, \\
x_2^E = \frac{\sum_{i=1}^{2}(m_i - m_{i-1})x_i}{m_2 - 1}, \\
\vdots \\
x_{N-1}^E = \frac{\sum_{i=1}^{N-1}(m_i - m_{i-1})x_i}{m_{N-1} - 1}.
\end{cases}
\tag{4}
$$

From (4), one can deduce all positive equilibria x_i^E $(i = 2, 3, \ldots, N-1)$ based on the given x_i and slopes m_i $(i = 0, 1, \ldots, N-1)$. Obviously, system (1) with (2) can be classified into several different linear regions based on the linear regions of its characteristic function. Figs. 2(a) and (b) show the linear regions of the characteristic functions of 3- and 4-scroll hyperchaotic attractors, respectively, where $\pm D_i$ $(i = 0, 1, \ldots, N-1)$ denotes different linear regions, $\pm x_i$ $(i = 1, \ldots, N-1)$ are the switching points, and $\pm x_i^E$ $(i = 0, 1, \ldots, N-1)$ are the equilibrium points.

Since system (1) with (2) is a piecewise-linear system, its dynamical behaviors are completely determined by several basic linear systems. Moreover, the stability of above linear systems is determined by the stability of the corresponding equilibrium points $\pm x_i^E$ $(i = 0, 1, \ldots, N-1)$. Obviously, the Jacobian at equilibria $\pm x_i^E$ $(i = 0, 1, \ldots, N-1)$ is given by

$$
J_i = \begin{bmatrix}
-\alpha m_i & \alpha m_i & -\alpha & 0 \\
\beta m_i & -\beta m_i & 0 & -\beta \\
\gamma_0 & 0 & \gamma_0 & 0 \\
0 & \gamma & 0 & 0
\end{bmatrix}.
\tag{5}
$$

For 3-scroll case, $x_0^E \in D_0$ and its eigenvalues are given by $\lambda_1 = -65.5816$, $\lambda_2 = 0.4479$, $\lambda_{3,4} = 0.0669 \pm j2.0200$; $\pm x_1^E \in \pm D_1$ and their eigenvalues are described by $\lambda_1 = 15.8866$, $\lambda_2 = 1.4570$, $\lambda_{3,4} = 0.6281 \pm j2.0667$; $\pm x_2^E \in \pm D_2$ and their eigenvalues are given by $\lambda_1 = -65.5816$, $\lambda_2 = 0.4479$, $\lambda_{3,4} = 0.0669 \pm j2.0200$. Therefore, equilibria x_0^E, $\pm x_2^E$ are saddle points with index 3 which generate three scrolls in regions D_0, $\pm D_2$, respectively. Moreover, equilibria $\pm x_1^E$ are unstable since they are divergence in regions $\pm D_1$, respectively.

Similarly, for 4-scroll case, $x_0^E \in D_0$ and its eigenvalues are given by $\lambda_1 = 13.3718$, $\lambda_2 = 1.6464$, $\lambda_{3,4} = 0.6909 \pm j2.0386$; $\pm x_1^E \in \pm D_1$ and their eigenvalues are described by $\lambda_1 = -63.3670$, $\lambda_2 = 0.4414$, $\lambda_{3,4} = 0.0628 \pm j2.0179$; $\pm x_2^E \in \pm D_2$ and their eigenvalues are given by $\lambda_1 = 13.3718$, $\lambda_2 = 1.6464$, $\lambda_{3,4} = 0.6909 \pm j2.0386$; $\pm x_3^E \in \pm D_3$ and their eigenvalues are described by $\lambda_1 = -63.3670$, $\lambda_2 = 0.4414$, $\lambda_{3,4} = 0.0628 \pm j2.0179$. Hence, equilibria $\pm x_1^E$, $\pm x_3^E$ are sad-
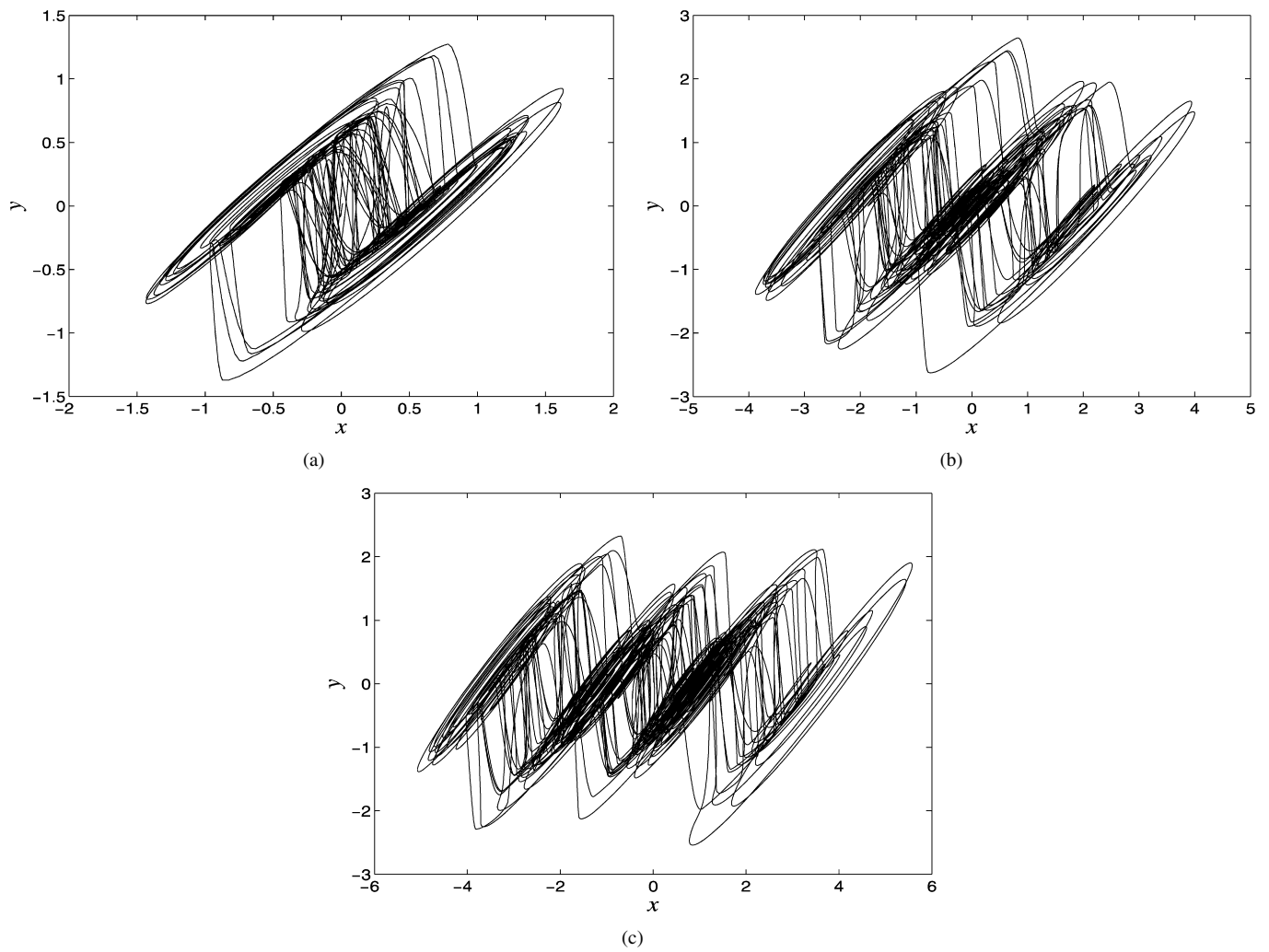
Fig. 1. Numerical simulations of hyperchaotic *n*-scroll attractors: (a) 2-scroll; (b) 3-scroll; (c) 4-scroll.
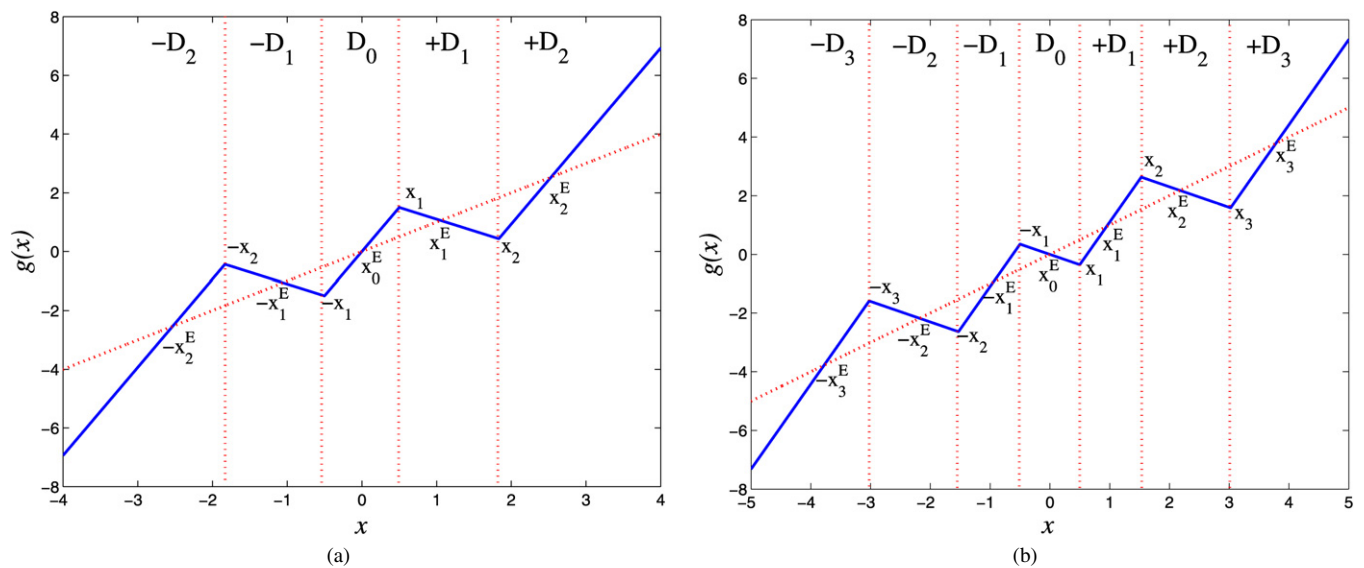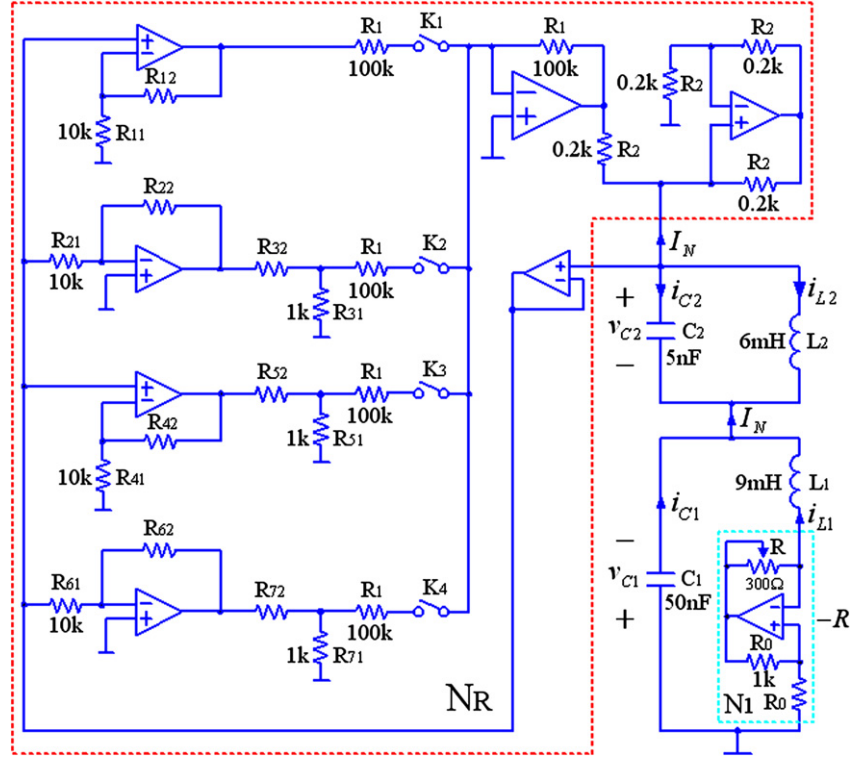

Fig. 2. Characteristic distribution regions of hyperchaotic *n*-scroll attractors: (a) 3-scroll; (b) 4-scroll.

Fig. 3. Circuit diagram for realizing hyperchaotic n-scroll attractors.

dle points with index 3 which generate four scrolls in regions $\pm D_1$, $\pm D_3$, respectively. Furthermore, equilibria x_0, $\pm x_2^E$ are unstable since they are divergence in regions D_0, $\pm D_2$, respectively.

3. Circuit realization of hyperchaotic n-scroll attractors

In the following, one constructs a circuit diagram to experimentally verify the hyperchaotic 2-, 3-, 4-scroll attractors. The circuit diagram is designed and its dynamic equation is rigorously derived from Fig. 3.

Fig. 3 shows the circuit diagram, where N_1 is the generator of the negative resistor $-R$, and N_R is the multi-PWL function generator satisfying $I_N = f(v_{C_2} - v_{C_1})$. All operational amplifiers are selected as Type TL082. All resistors are exactly adjustable resistors or potentiometers. The voltage of the electric source is $E = 15$ V. Thus, the saturating voltages of the operation amplifiers are $E_{\text{sat}} = 14.3$ V.

According to Fig. 3, the circuit equation is derived as follows:

$$\begin{cases} C_1 \frac{dv_{C_1}}{dt} = f(v_{C_2} - v_{C_1}) - i_{L_2}, \\ C_2 \frac{dv_{C_2}}{dt} = -f(v_{C_2} - v_{C_1}) - i_{L_2}, \\ L_1 \frac{di_{L_1}}{dt} = v_{C_1} + R i_{L_1}, \\ L_2 \frac{di_{L_2}}{dt} = v_{C_2}, \end{cases} \tag{6}$$

where $f(v_{C_2} - v_{C_1}) = G_{N-1}(v_{C_2} - v_{C_1}) + 0.5 \sum_{i=1}^{N-1}(G_{i-1} - G_i)(|v_{C_2} - v_{C_1} + E_i| - |v_{C_2} - v_{C_1} - E_i|)$ is a piecewise-linear characteristic function.

Comparing (1) with (6), then one gets the transformation relationship of parameters:

$$\begin{cases} \tau_0 = 2RC_1, \quad \tau = \frac{t}{\tau_0}, \quad \alpha = 2, \quad \beta = \frac{2C_1}{C_2} = 20, \\ \gamma_0 = \frac{2R^2 C_1}{L_1} = 1, \quad \gamma = \frac{2R^2 C_1}{L_2} = 1.5, \\ x = \frac{v_{C_1}}{V_{\text{BP}}}, \quad y = \frac{v_{C_2}}{V_{\text{BP}}}, \quad z = \frac{R i_{L_1}}{V_{\text{BP}}}, \quad w = \frac{R i_{L_2}}{V_{\text{BP}}}, \\ V_{\text{BP}} = 1 \text{ V}, \quad G_i = m_i G \quad (i = 0, 1, 2, \ldots), \quad G = \frac{1}{R}, \\ g(y - x) = R f(v_{C_2} - v_{C_1}), \end{cases} \tag{7}$$

where $\frac{1}{\tau_0} = \frac{1}{2RC_1}$ is the time-scale transformation factor.

From (7), one has the parameters: $L_1 = 9$ mH, $L_2 = 6$ mH, $C_1 = 50$ nF, $C_2 = 5$ nF, $R = 300$ Ω. Then one can get the theoretical values of resistors based on the given parameters as follows:

(1) For hyperchaotic 2-scroll attractor:

$$\begin{cases} G_0 = \frac{m_0}{R} = -0.67 \text{ mS}, \\ G_1 = \frac{m_1}{R} = 10 \text{ mS}, \\ E_1 = x_1 V_{\text{BP}}, \\ r_1 = \frac{R_{12}}{R_{11}} = G_1 R_2 - 1 = 1.00, \\ r_2 = \frac{R_{22}}{R_{21}} = \frac{E_{\text{sat}}}{E_1} = 28.6, \\ r_3 = \frac{R_{32}}{R_{31}} = \frac{r_2}{R_2(G_1 - G_0)} - 1 = 12.4. \end{cases} \tag{8}$$

(2) For hyperchaotic 3-scroll attractor:

$$\begin{cases} G_0 = \frac{m_0}{R} = 10 \text{ mS}, \quad G_1 = \frac{m_1}{R} = -2.7 \text{ mS}, \\ G_2 = \frac{m_2}{R} = 10 \text{ mS}, \quad E_i = x_i V_{BP} \quad (i = 1, 2), \\ r_1 = \frac{R_{12}}{R_{11}} = G_2 R_2 - 1 = 1.00, \\ r_2 = \frac{R_{22}}{R_{21}} = \frac{E_{sat}}{E_2} = 7.80, \\ r_3 = \frac{R_{32}}{R_{31}} = \frac{r_2}{R_2(G_2 - G_1)} - 1 = 2.08, \\ r_4 = \frac{R_{42}}{R_{41}} = \frac{E_{sat}}{E_1} - 1 = 27.60, \\ r_5 = \frac{R_{52}}{R_{51}} = -\frac{1+r_4}{R_2(G_1 - G_0)} - 1 = 10.29. \end{cases} \quad (9)$$

(3) For hyperchaotic 4-scroll attractor:

$$\begin{cases} G_0 = \frac{m_0}{R} = -2.3 \text{ mS}, \quad G_1 = \frac{m_1}{R} = 9.7 \text{ mS}, \\ G_2 = \frac{m_2}{R} = -2.3 \text{ mS}, \quad G_3 = \frac{m_3}{R} = 9.7 \text{ mS}, \\ E_i = x_i V_{BP} \quad (i = 1, 2, 3), \\ r_1 = \frac{R_{12}}{R_{11}} = G_3 R_2 - 1 = 0.93, \\ r_2 = \frac{R_{22}}{R_{21}} = \frac{E_{sat}}{E_3} = 4.73, \\ r_3 = \frac{R_{32}}{R_{31}} = \frac{r_2}{R_2(G_3 - G_2)} - 1 = 0.97, \\ r_4 = \frac{R_{42}}{R_{41}} = \frac{E_{sat}}{E_2} - 1 = 8.35, \\ r_5 = \frac{R_{52}}{R_{51}} = -\frac{1+r_4}{R_2(G_2 - G_1)} - 1 = 2.90, \\ r_6 = \frac{R_{62}}{R_{61}} = \frac{E_{sat}}{E_1} = 28.6, \\ r_7 = \frac{R_{72}}{R_{71}} = \frac{r_6}{R_2(G_1 - G_0)} - 1 = 10.90. \end{cases} \quad (10)$$

Note that capacitance C_1 in Fig. 3 connects to the earth. To exactly adjust C_1, one introduces the equivalent capacitance as shown in Fig. 4. According to the circuit theory, $C_1 = \frac{R_2 R_4 C_5}{R_1 R_3}$. Therefore, it is very easy to adjust the capacitance C_1 by tuning the adjustable resistors R_1, R_2, R_3, R_4.

Let $R_1 = 100$ kΩ, $R_2 = 0.2$ kΩ, $R_{31} = R_{51} = R_{71} = 1$ kΩ, $R_{11} = R_{21} = R_{41} = R_{61} = 10$ kΩ. Comparing Fig. 3 with system (1) under (2), one can calculate the resistors R_{n2} ($1 \leqslant n \leqslant 7$) as shown in Tables 1 and 2. As seen from Fig. 3, when K_1, K_2 are switched on and K_3, K_4 are switched off, the circuit diagram can create a hyperchaotic double-scroll attractor as shown in Fig. 5(a); when K_1, K_2, K_3 are switched on and K_4 is switched off, the circuit diagram can generate a hyperchaotic 3-scroll attractor as shown in Fig. 5(b);

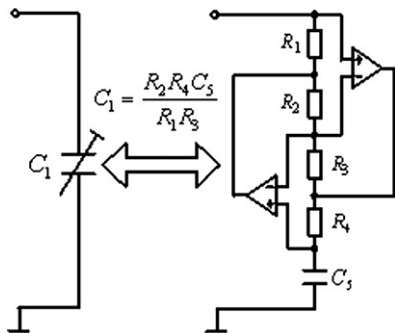
Fig. 4. Equivalent circuit diagram of adjustable capacitance C_1.

Table 1
The ratios of the resistors $r_n = \frac{R_{n2}}{R_{n1}}$ ($1 \leqslant n \leqslant 7$) and the number of the scrolls N

r_1	r_2	r_3	r_4	r_5	r_6	r_7	N
1.00	28.60	12.40					2
1.00	7.80	2.08	27.60	10.29			3
0.93	4.73	0.97	8.35	2.90	28.60	10.90	4

Table 2
The resistors $R_{n2} = r_n R_{n1}$ ($1 \leqslant n \leqslant 7$) and the number of the scrolls N

R_{12}	R_{22}	R_{32}	R_{42}	R_{52}	R_{62}	R_{72}	N
10k	286k	12.4k					2
10k	78k	2.08k	276k	10.29k			3
9.3k	47.3k	0.97k	83.5k	2.90k	286k	10.9k	4

when K_1, K_2, K_3, K_4 are switched on, the circuit diagram can create a hyperchaotic 4-scroll attractor as shown in Fig. 5(c).

4. DSP realization of hyperchaotic n-scroll attractors

This section proposes a novel DSP method to physically realize hyperchaotic 2-, 3-, 4-scroll attractors.

DSP is a special real time and fast digital signal processing device. There are several different kinds of DSP series, such as DSP2000 series, DSP5000 series, and DSP6000 series. Since DSP concentrates the advanced digital signal processing technology and the micro-electronic technology into a small chip, it has been widely applied to the communication, signal processing, and industry control fields.

Here, one uses DSP2812 device with one TMS320F2812 chip and four D/A converters to generate hyperchaotic multi-scroll signals. DSP2812 has two prominent characteristics: (1) it has four D/A transformation devices which can simultaneously transform four routes of digital signals into the corresponding four routes of analog signals; (2) its highest frequency is 150 MHz which is enough to satisfy the requirement of our experiments.

To create high quality hyperchaotic signal from DSP2812, one needs to transform continuous time signal into discrete time signal and then do extended transformation. According to system (1), the discrete difference equation is described by

$$\begin{cases} x(n) = \Delta T \cdot \alpha \{g[y(n-1) - x(n-1)] - z(n-1)\} \\ \quad\quad + x(n-1), \\ y(n) = \Delta T \cdot \beta \{-g[y(n-1) - x(n-1)] - w(n-1)\} \\ \quad\quad + y(n-1), \\ z(n) = \Delta T \cdot \gamma_0 [x(n-1) + z(n-1)] + z(n-1), \\ w(n) = \Delta T \cdot \gamma y(n-1) + w(n-1), \end{cases} \quad (11)$$

where $\alpha = 2$, $\beta = 20$, $\gamma_0 = 1$, $\gamma = 1.5$, and ΔT is the sampling time which is determined by the original chaotic equation. Here, $\Delta T = 0.03$. From (2), the discrete characteristic function
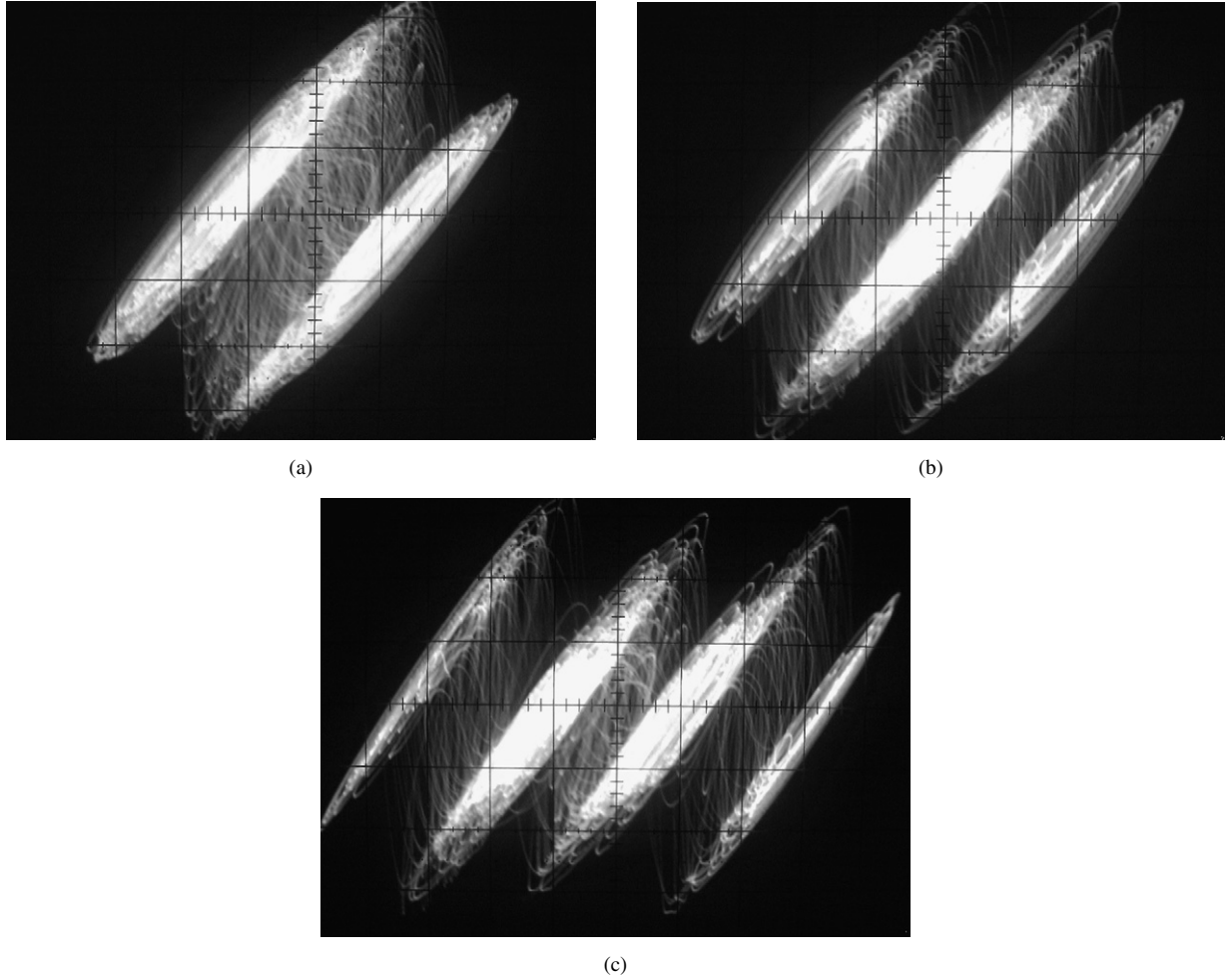
(a)

(b)

(c)

Fig. 5. Experimental observations of hyperchaotic n-scroll attractors: (a) 2-scroll, where $x = 0.5$ V/div, $y = 0.4$ V/div; (b) 3-scroll, where $x = 1.0$ V/div, $y = 0.7$ V/div; (c) 4-scroll, where $x = 1.3$ V/div, $y = 0.7$ V/div.

is given by

$$
\begin{aligned}
g\big[y(n-1) &- x(n-1)\big] \\
&= m_{N-1}\big[y(n-1) - x(n-1)\big] \\
&+ 0.5 \sum_{i=1}^{N-1} (m_{i-1} - m_i)\big(\big|y(n-1) - x(n-1) + x_i\big| \\
&\quad - \big|y(n-1) - x(n-1) - x_i\big|\big),
\end{aligned} \tag{12}
$$

where m_i $(i = 0, 1, \ldots, N-1)$ are the slopes of the linear regions of characteristic function $g(\cdot)$, x_i $(i = 2, 3, \ldots, N-1)$ are the switching points of characteristic function $g(\cdot)$.

To improve the calculating precise of DSP2812, one needs to do the extended transformation: $u = kx$, $v = ky$, $s = kz$, $q = kw$, where $k > 1$ is the expanding ratio. According to (11) and (12), one has

$$
\begin{cases}
u(n) = \Delta T \cdot \alpha\{g[v(n-1) - u(n-1)] - s(n-1)\} \\
\qquad + u(n-1), \\
v(n) = \Delta T \cdot \beta\{-g[v(n-1) - u(n-1)] - q(n-1)\} \\
\qquad + v(n-1), \\
s(n) = \Delta T \cdot \gamma_0[u(n-1) + s(n-1)] + s(n-1), \\
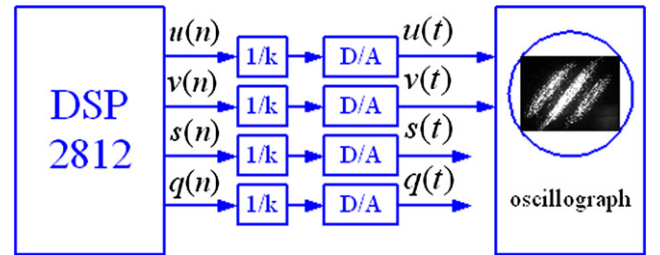q(n) = \Delta T \cdot \gamma v(n-1) + q(n-1)
\end{cases} \tag{13}
$$

Fig. 6. DSP2812 working principle diagram for realizing hyperchaotic n-scroll attractors.

and

$$
\begin{aligned}
g\big[v(n-1) &- u(n-1)\big] \\
&= m_{N-1}\big[v(n-1) - u(n-1)\big] \\
&+ 0.5 \sum_{i=1}^{N-1} (m_{i-1} - m_i)\big(\big|v(n-1) - u(n-1) + kx_i\big| \\
&\quad - \big|v(n-1) - u(n-1) - kx_i\big|\big),
\end{aligned} \tag{14}
$$

where $k = 30$.

Fig. 6 shows the DSP2812 working principle diagram for realizing hyperchaotic n-scroll attractors. The detailed working
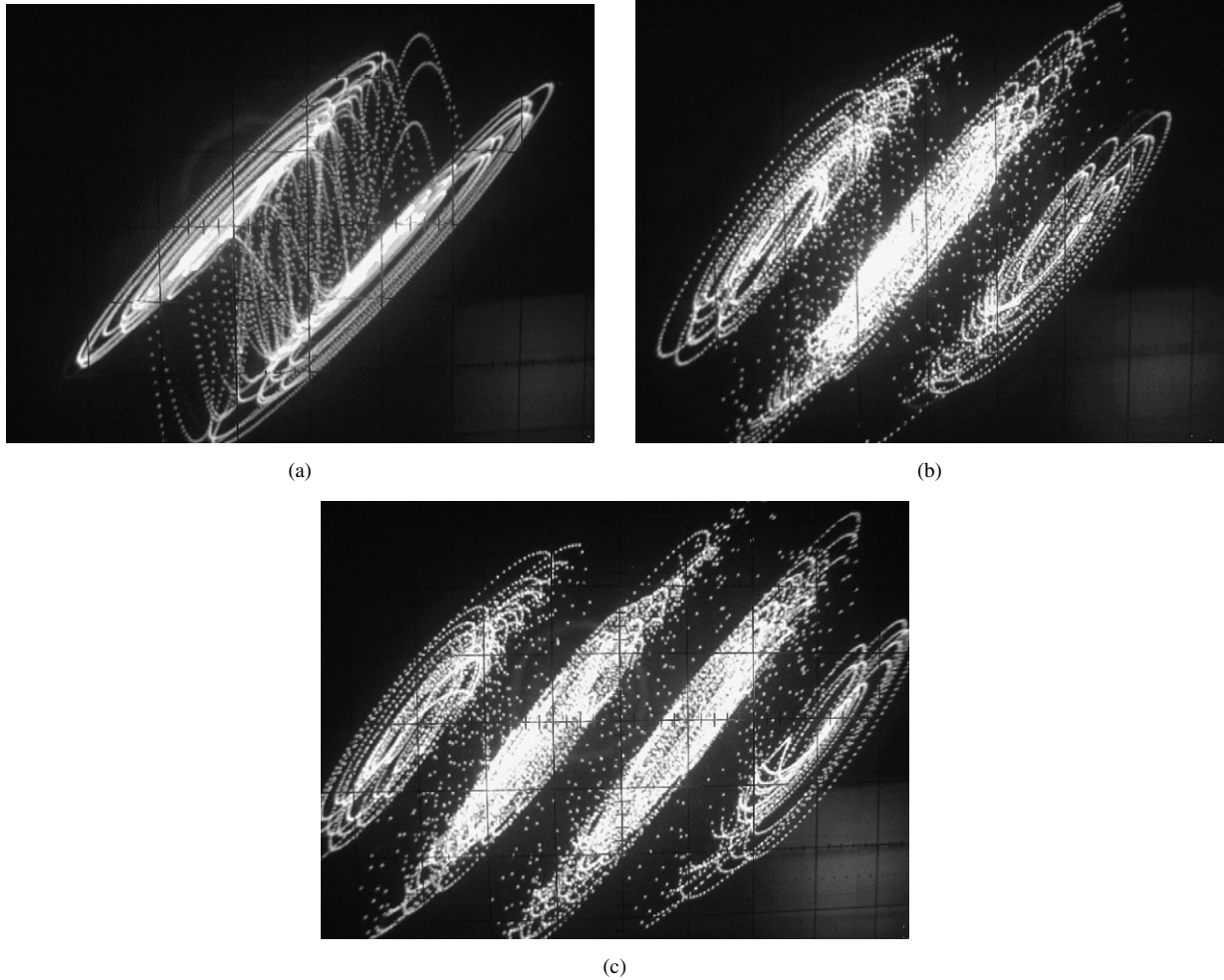
(a)

(b)

(c)

Fig. 7. DSP2812 realization of hyperchaotic n-scroll attractors: (a) 2-scroll, where $x = 0.5$ V/div, $y = 0.4$ V/div; (b) 3-scroll, where $x = 1.0$ V/div, $y = 0.7$ V/div; (c) 4-scroll, where $x = 1.3$ V/div, $y = 0.7$ V/div.

process can be summarized as follows: (1) generate iterative series $u(n)$, $v(n)$, $s(n)$, $q(n)$ from (13) and (14), where the initial values are given by $u(0) = 0.01$, $v(0) = 0.02$, $s(0) = 0.02$, $q(0) = 0.01$; (2) do the compressed transformation $u' = \frac{1}{k}u$, $v' = \frac{1}{k}v$, $s' = \frac{1}{k}s$, $q' = \frac{1}{k}q$ since the linear dynamic regions of D/A transformation devices are limited by $[-15$ V$, 15$ V$]$; (3) transform the digital signals $u'(n)$, $v'(n)$, $s'(n)$, $q'(n)$ into the analog signals $u(t)$, $v(t)$, $s(t)$, $q(t)$ via D/A transformation devices in DSP2812.

Fig. 7 shows the experimental observations of the hyperchaotic 2-, 3-, 4-scroll attractors in the oscillograph of DSP2812. Similarly, our experimental results show that the DSP realization has a certain robustness against the variation of all system parameters of all devices, the sampling time ΔT and the extending ration k.

5. Conclusions

This Letter has proposed a novel block circuit diagram for the hardware implementation of hyperchaotic 2-, 3-, 4-scroll attractors from a generalized MCK circuit. Furthermore, a novel DSP method is presented for physically realizing the above

hyperchaotic 2-, 3-, 4-scroll attractors by using appropriate discrete and extended transformations. In addition, the derived recursive formulas of system parameters provide a theoretical basis for the physical realization of the hyperchaotic attractors with a large number of scrolls. This is the first time in the literature to report the experimental verification of hyperchaotic 3- and 4-scroll attractors.

References

[1] J. Lü, S.C. Zhang, Phys. Lett. A 286 (2001) 148.
[2] H. Wang, G. Chen, J. Lü, Phys. Lett. A 333 (2004) 246.

[3] J. Lü, G. Chen, Int. J. Bifur. Chaos 12 (2002) 659.

[4] L.O. Chua, J. Circuits Systems Comput. 4 (1994) 117.

[5] M.E. Yalcin, J.A.K. Suykens, J. Vandewalle, in: Proceedings of the IEEE Workshop on Nonlinear Dynamics of Electronic Systems, Catania, Italy, 2000, p. 25.

[6] S.M. Yu, Z.G. Ma, S.S. Qiu, S.G. Peng, Q.H. Lin, Chin. Phys. 13 (2004) 317.

[7] M. Itoh, T. Yang, L.O. Chua, Int. J. Bifur. Chaos 9 (1999) 1393.

[8] M.E. Yalcin, J.A.K. Suykens, J. Vandewalle, IEEE Trans. Circuits Systems I 47 (2000) 425.

[9] D.A. Miller, G. Grassi, IEEE Trans. Circuits Systems I 48 (2001) 366.

[10] M.E. Yalcin, J.A.K. Suykens, J. Vandewalle, S. Ozoguz, Int. J. Bifur. Chaos 12 (2002) 23.

[11] M.E. Yalcin, J.A.K. Suykens, J.P.L. Vandewalle, Cellular Neural Networks, Multi-Scroll Chaos and Synchronization, World Scientific, Singapore, 2005.

[12] G. Zhong, K.F. Man, G. Chen, Int. J. Bifur. Chaos 12 (2002) 2907.

[13] J. Lü, G. Chen, D.Z. Cheng, S. Celikovsky, Int. J. Bifur. Chaos 12 (2002) 2917.

[14] F. Han, J. Lü, X. Yu, G. Chen, Y. Feng, Dynamics Continuous Discrete Impulsive Systems Ser. B 12 (2005) 95.

[15] J. Lü, T. Zhou, G. Chen, X. Yang, Chaos 12 (2002) 344.

[16] J. Lü, X. Yu, G. Chen, IEEE Trans. Circuits Systems I 50 (2003) 198.

[17] J. Lü, F. Han, X. Yu, G. Chen, Automatica 40 (2004) 1677.

[18] J. Lü, G. Chen, X. Yu, H. Leung, IEEE Trans. Circuits Systems I 51 (2004) 2476.

[19] S.M. Yu, J. Lü, H. Leung, G. Chen, IEEE Trans. Circuits Systems I 52 (2005) 1459.

[20] J. Lü, S.M. Yu, H. Leung, G. Chen, IEEE Trans. Circuits Systems I 53 (2006) 149.

[21] J. Lü, G. Chen, Int. J. Bifur. Chaos 16 (2006) 775.

[22] C.W. Wu, Synchronization in Coupled Chaotic Circuits and Systems, World Scientific, Singapore, 2002.

[23] T. Matsumoto, L.O. Chua, T. Kobayashi, IEEE Trans. Circuits Systems I 33 (1986) 828.